BIODIVERSITAS
Volume 23, Number 8, August 2022
Pages: 4272-4282

ISSN: 1412-033X
E-ISSN: 2085-4722
DOI: 10.13057/biodiv/d230851

Morpho-anatomical characterization and DNA barcoding analysis of *Pluchea indica* (L.) Less.

DWI KUSUMA WAHYUNI[1,2,♥], SITI RIZQIYATUL MUKARROMAH[1], PUTUT RAKHMAD[1], MOCHAMMAD ILHAM[1], GALUH AYU RAKASHIWI[1], DANI TRI INDRIATI[1], BRUNY FLARANDA YOKU[1], HERY PURNOBASUKI[1], JUNAIRIAH[1], SEHANAT PRASONGSUK[1,2,♥♥]

[1]Department of Biology, Faculty of Science and Technology, Universitas Airlangga. Jl. Dr. Ir. H. Soekarno, Mulyorejo, Surabaya 60115, East Java, Indonesia. Tel./fax.: +62- 31-5914042, ♥email: dwi-k-w@fst.unair.ac.id

[2]Plant Biomass Utilization Research Unit, Department of Botany, Faculty of Science, Chulalongkorn University. 254 Phaya Thai Rd, Bangkok, 10330, Thailand. ♥♥email: sehanat.p@chula.ac.th

Manuscript received: 27 December 2022. Revision accepted: 2 August 2022.

Abstract. *Wahyuni DK, Mukarromah SR, Rakhmad P, Ilham M, Rakashiwi GA, Indriati DT, Yoku BF, Purnobasuki H, Junairiah, Prasongsuk S. 2022. Morpho-anatomical characterization and DNA barcoding analysis of* Pluchea indica *(L.) Less.. Biodiversitas 23: 4272-4282. Pluchea indica* (L.) Less. is a member of the Asteraceae family and is popular as a medicinal plant. It is very important to authenticate plants using various markers to confirm the labeling of plants and to reveal the bioactive compounds for pharmaceutical research. This study aims to characterize the morpho-anatomical and DNA barcoding aspects of *P. indica*. Three samples obtained from Taman Husada Graha Famili, Surabaya, Indonesia were used in this study. Morphological studies were carried out descriptively, while the paraffin method was used for anatomical observations. DNA barcoding analysis was performed by amplifying and aligning the *rbcL* and *matK* genes. Morphologically, *P. indica* has organs like Asteraceae plants in general, with specific characteristics in leaves and flowers. *P. indica* has an anatomical organ similar to that of Asteraceae plants globally, only that there are specific histological features on its leaves, including anomocytic stomata, glandular cells, and multicellular glandular trichomes. Alignment and reconstruction of the phylogenetic tree showed that the sample plants were closely related to *P. indica* in the GenBank database. Based on morpho-anatomical characters and DNA barcodes, the plant under study was confirmed as *P. indica* L. (Less).

Keywords: DNA barcode, *matK*, morpho-anatomy, *Pluchea indica* L. (Less.), *rbcL*

INTRODUCTION

Pluchea indica (L.) Less. is a plant of the Asteraceae family that has health benefits, such as anti-inflammatory (Srisook et al. 2021), antioxidant (Suriyaphan 2014; Sugiaman et al. 2021; Srisook et al. 2021), antibacterial activity, and anti-cancer properties (Chan et al. 2022). These benefits are due to the content of various secondary metabolites, such as caffeoylquinic acid, phenolic acid, flavonoids, and thiophene (Chan et al. 2022). Concerning the pharmaceutical aspect, *P. indica* strengths are also related to its high viability. This plant will adapt to varied environmental conditions by making anatomically and morphologically changes (De Mico and Aronne 2012; Mandel et al. 2019).

Herbal plants are used as an alternative to synthetic medicine. Nowadays the active substances in plants are used as models to produce many drugs (Veeresham 2012). The phytopharmaceutical industry applies standards that must be met, one of which is the use of appropriate herbal plant species. Morphological approaches are commonly used to identify plant species (Kaur and Singh 2020). However, these markers have drawbacks such as environmental conditions and subjective errors when documenting and recording data (Gratani 2014; Hong et al. 2021). In addition, macro-morphological similarities can occur between plant species within the same genus (Berlin 2014). Consequently, relying on morphological characteristics alone can cause plant specimens to be mislabeled (De Boer et al. 2014). Mislabeling specimens can reduce therapeutic effectiveness and harm consumers (Michel et al. 2016).

Anatomical markers can also be used to determine the content of secondary metabolites for pharmaceutical purposes, such as trichomes. Several Asteraceae species have trichomes containing terpenoids, alkaloids, phenols, and oils (Dorly et al. 2015). Mercado et al. (2021) reported that *Artemisia copa* has schizogenous secretory ducts distributed in the leaf midvein and cortex in the stem. However, the use of anatomical markers alone will not be sufficient to produce maximum taxonomic data, because these markers also depend on environmental factors (Zagoto and Violita 2019).

A molecular approach, such as DNA barcoding develops into conclusive authentication and taxonomic assignment for phyto preparation quality assurance (Ulrich-Merzenich et al. 2007; Patwardhan et al. 2014). DNA barcoding is a taxonomic method in which a short genetic marker identifies the DNA of which organisms or a particular species (Sarvananda 2018). DNA barcoding is a powerful and efficient tool for identifying poorly studied species (Genievskaya et al. 2017; Kress 2017). There are seven candidate DNA plastid markers, namely the *atpF-atpH*, *matK*, *rbcL*, *rpoB*, *rpoC1*, *psbK-psbI*, and *trnH-psbA*.

However, based on various assessment criteria, the recommended DNA barcode for plants combines *rbcL* and *matK* loci (CBOL Plant Working Group 2009). According to Kress et al. (2009), the combination of *rbcL* and *matK* could discriminate >98% of Angiosperm species from a forest on Panama's Barro Colorado Island. DNA barcoding study *of Pluchea indica* was used to evaluate the mangrove diversity in China (Mao et al. 2021) using primers *rbcL* and *matK*. Both genes were also applied for the DNA barcoding study of *P. carolinensis* and *P. odorata* in the Rio Grand Valley of Texas (de Alba 2015).

In order for the medical potential of *P. indica* to be maximally known, especially in terms of the distribution of its bioactive components, it is necessary to observe using various markers so that the data obtained are not biased. This study aims to identify *P. indica* using a morpho-anatomical approach and DNA barcoding. It is hoped that the results of this study can be used as a reference for future pharmaceutical activities.

MATERIALS AND METHODS

Plant materials

Three individuals of *Pluchea indica* L. (Less.) in Taman Husada Graha Famili, Surabaya, Indonesia were used in this study. All materials have been identified by staff from Purwodadi Botanical Garden, National Research and Innovation Agency, and the voucher specimen was deposited in the Plant Systematics Laboratory, Biology Department, Faculty of Science, Universitas Airlangga, Surabaya (Voucher No. PI01102021, PI02102021, and PI03102021).

Procedures

Morpho-anatomical characterization

Morphological data including vegetative and generative organs were described based on voucher specimens from Taman Husada Graha Famili, Surabaya. Vegetative organs will be processed using the paraffin method for anatomical investigations. This method includes several stages, such as collecting plants from the field, washing, fixing, dehydrating, dealcoholizing, infiltrating, blocking in pure paraffin, slicing, gluing, staining, and covering (Santos et al. 2016; Susetyarini et al. 2020). The safranin and fast green were used for plant tissue staining (Purnobasuki et al. 2017). The anatomical characters such as tissue type, secretory cells, and other discriminate characters were described and analyzed. Anatomical preparations were observed using a light microscope with a magnification of 200-400x.

DNA extraction and amplification

Total genomic DNA was isolated from 0.1 g of young leaves using the Plant DNA Genomic Kit (Tiangen, China). The isolated DNA was verified the purity and concentration using the SkanIt computer program of Thermo Scientific Multiskan Go at 260 nm and 280 nm. The solution used as a blank is TE buffer.

Polymerase chain reaction (PCR) amplification of *rbcL* and *matK* genes was carried out using primers that were specially designed for the Asteraceae, namely the *rbcL* primers (Forward: AAG-TTC-CTC-CAC-CGA-ACT-GTA-G; Reverse: TAC-TGC-GGG-TAC-ATG-CGA-AG) and the *matK* primers (Forward: TGG-TTC-AGG-CTC-TTC-GCT-ATT-G; Reverse: CTG-ATA-AAT-CGG-CCC-AAA-TCG-C) (Do et al. 2019). PCR mixtures were performed in a volume of 35 µL containing the mixture consisting of 17.5 µL GoTaq® Green Master Mix, 1.5 µL of each forward and reverse primer with a concentration of 350-500 nM, 50 ng DNA template (5 µL), and 9.5 µL of nuclease-free water. The PCR program was adjusted into 5 stages, including pre-denaturation at 94°C for 5 minutes at one cycle, 35 cycles for denaturation at 94°C for 30 seconds, annealing at 56°C for 45 seconds, and extension at 72°C for 45 seconds, final extension at 72°C for 5 minutes at one cycle, and soaking at 4°C. PCR reactions were performed in an Eppendorf® master cycler personal.

Electrophoresis and sequencing

PCR was confirmed using electrophoresis on 1% agarose gel (Promega, USA). Electrophoresis results were checked using a UV transilluminator to determine whether DNA amplification bands were formed or not (Wahyuni et al. 2019). After verification of the success of PCR amplification, the reaction volumes were scaled up to 50 µL for sequencing. Then, PCR products were sent to the 1st Base Sequencing Service (Singapore) for sequencing. *P. indica* plant used in this study was registered in the GenBank database with accessions ON685207, ON685208, and ON685209 for the *rbcL* locus, while accessions ON685204, ON685205, and ON685206 for the *matK* locus.

Data analysis

Morpho-anatomical characters of roots, stems, leaves, and flowers were analyzed descriptively. DNA sequence alignment was performed using the rapid identification tool BLAST (Basic Local Alignment Search Tool) online at https://blast.ncbi.nlm.nih.gov. Then DNA sequence data were processed using Bioedit (Yang et al. 2017) and Mega X software to reconstruct the phylogenetic tree (Kumar et al. 2018). The data used to construct the phylogenetic tree were from three replicates of *P. indica* sequences and 9 sequences of plant data in the GenBank database. The closest relatives to sample sequences from each gene were also aligned with ClustalW using BioEdit (Yang et al. 2017). Reconstruction of the phylogenetic tree using three scenarios, namely trees based on *rbcL*, *matK*, and a combination of *rbcL+matK*. The phylogenetic tree was built using MEGA software with a maximum-likelihood tree model (Tamura et al. 2021). A cluster analysis was conducted using the distance method UPGMA (Unweighted Pair-Group Method with Arithmetic Mean). The fittest model was chosen based on the lowest Bayesian Information Criterion (BIC) value.

RESULTS AND DISCUSSION

Morphological characterization

Based on morphological observation, *P. indica* is a perennial shrub (Figures $1A_{1-2}$) that grows upright with a height of up to 2 m tall (Hunger 1997; Peng et al. 1998;

Wahyuni et al. 2016; Chan et al. 2022). The species has a taproot system with many branching brownish roots (ramosus) (Figure 1B) as well as Asteraceae members (Wahyuni et al. 2016). The taproot would be continuously growing as well as the root branching. In relation to the function of the root, there are two kinds of root branching, i.e. (1) an actively growing root characterized by the fresh brown-yellowish color and (2) an un-actively growing root characterized by the brown whitish color. The stems were round with the direction of growing perpendicular (erectus) and shape of the stems was round (teres). The type of stem was the woody stem (lignosus) (Figure 1C). However, the young stem is herbaceous and pilosus with alternate phyllotaxis and monopodial branching (Figure 1D) (Susetyarini et al. 2020).

Leaves alternate arranged (Figure 1D), single (folium simplex), short-stalked, light green when young to dark green when mature, an oval breech shape (obovatus), a pointed leaf tip (acutus), serrated leaf edge, and a tapered leaf base (acutus) as a major character of ovoid leaf. The lamina was wider at the tip (Simpson 2006). The venation was pinnate leaf bones (penninervis), starting from the basic to the tip, ramify to the leaf edge as finfish (Figure $1E_{1-2}$). When leaves of this plant are crushed, it will emit an aromatic smell. In the genus *Pluchea*, obovoid leaf shape is a common characteristic (Peng et al. 1998).

Stems and leaves were covered by trichomes. There were many gland hairs in the young leaves compared to old leaves. The old leaves were almost covered by non-gland hairs. This result is supported by Susetyarini et al. (2020). Compared to individuals from Australia, the hairs of specimens studied here were finer around 0.1 mm (Hunger 1997).

The inflorescence of *P. indica* is capitulum type (Hunger 1997; Peng et al. 1998; Wahyuni et al. 2016; Susetyarini et al. 2020), because there are many flowers with completely reproductive properties (stamen and stigma in each flower). Composite flower supported by receptaculum and covered by bractea. The flower is a hump with a handle, the layout of the flower was flos terminals (Figure 1F) and comes from the axilla (flos axillaris). The marginal florets (filiform flower) are female, while the central florets are bisexual but functionally staminate (tube flower). Tube flowers are surrounded by calyx and corolla. The calyx is arranged in large numbers with a purplish white color, while the corolla is composed of 5 lobes that are tubular with color almost the same as the calyx. The pistil (stigma and style) has a higher position than the anther, both have a purple color, and only the color of the anther is darker (Figures 1G-J). Flowering occurs throughout the year (Chan et al. 2022). The color of corolla correlated to attract the insect for pollination (Wilson et al. 2017).

Fruits are top-shaped, ribbed, one-seeded, and indehiscent (Figures 1K-M). There were two kinds of seeds, i.e. (1) unfertile seed characterized by the seed was not growing and developing well, almost disappeared and covered by white pappus (Figure K), and (2) fertile seed with corolla, stigma, and stylus (Figures 1L and 1M). The size of seed is small and reproduction functionally, however generative reproduction of *Pluchea* is rare. This species is commonly propagated by stem grafting. Regularly pruning is very important to control the distribution of this species, because the small seed could spread and grow fast. This species distributes worldwide and is a very invasive plant species (Hunger 1997; https://www.cabi.org/isc/datasheet/116400).

Pluchea was separated from other members of the Asteraceae family because the achenes were not sericeous, capitula were less than 1 cm long, marginal florets were not ligulate, corolla was regularly lobed and the pappus was not rigid scalelike bristles. *P. indica* has two specific characters, i.e., shrub habitus, and obovate-shaped leaves. This species is closely related to *P. dunlopii*, especially in terms of leaf shape. Leaves of *P. indica* are 2-7 cm long with leaf shape obovate and acute, while *P. dunlopii* leaves have a length of 0.7-3 cm with an obtuse shape or sometimes truncate (Hunger 1997).

King-Jones (2001) revised members of the genus *Pluchea*, which turns out to have 7 species with cylindrical capitula as special characteristics. They were *P. rufescens*, *P. bojeri*, *P. grevei*, *P. indica*, *P. lanceolata*, *P. lycioides*, and *P. baccharoides*. The key characters of the *P. indica* were shrubby with sessile glands only, obovoid leaf, leaf base not decurrent, leaves 1-4 cm wide, capitula cylindrical, corolla of disc florets never hair, receptacle glabrous, pappus bristles not fused at base and style long bifid apical sweeping hairs obtuse.

Anatomical characterization

An anatomical study is required to understand the presence and location of cells that produce and store the secondary metabolites (Ilham et al. 2022). The cross-sectional anatomy of *P. indica* root shows several tissues, namely epidermis, collenchyma, cortex, endodermis, pericycle, and vascular tissue, which were clear and can be distinguished between the tissues (Figure $2A_{1-2}$). The epidermal tissue formation consists of a single layer of cells (uniseriate) that are tightly packed (Susetyarini et al. 2020). The general function of the epidermis is to protect the underlying tissue mechanically. The special function of this tissue is to regulate gas exchange between the environment and the inner tissue and reduce excessive water evaporation or water loss (Baas et al. 2015). Beneath the epidermis, there is collenchyma tissue which has the form of irregular cortical cells that are tightly packed and consist of several layers. This tissue is responsible for supporting the main growing organs, with thickened walls during and after elongation (Leroux 2012).

Inside of collenchyma is a cortex consisting of parenchyma cells, which have thin-walled characteristics with irregular shapes and are not tightly arranged. Between the cortex and the vascular tissue, two tissues have different functions, namely endodermis and pericycle. The endodermis root is the cylindrical boundary that separates the inner vascular tissue from the outer cortex and functions as an apoplasmic barrier for selective nutrient uptake (Miyashima and Nakajima 2011).

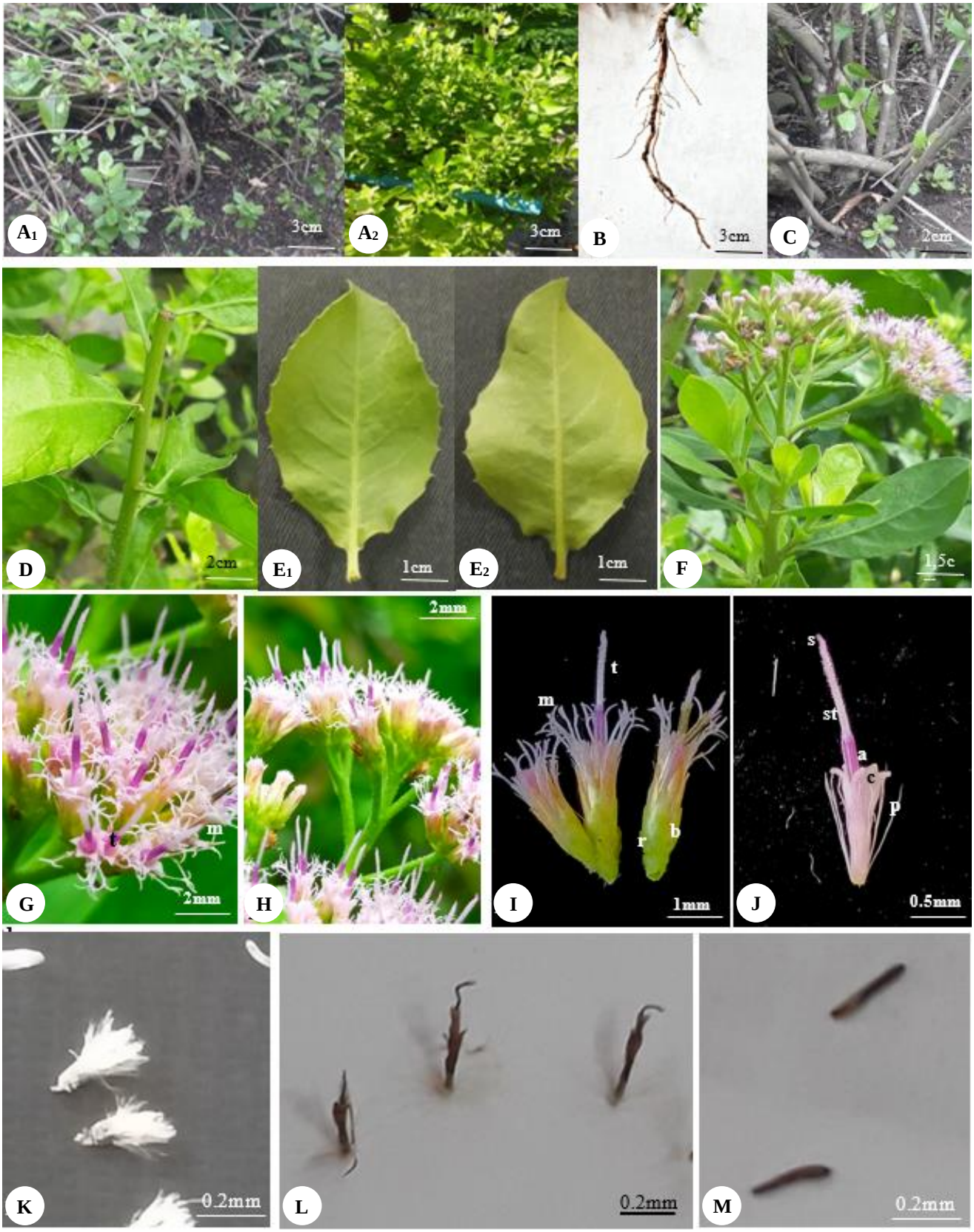

Figure 1. Morphology of *Pluchea indica* (L.) Less. A_1. Habit viewed from below, A_2. Habit viewed from above, B. Taproot, C. Lower stem, D. Upper stem, E_1. Adaxial leaf, E_2. Abaxial leaf, F. Inflorescences, G-H. Inflorescences in a corymb, I. Composite flower. r: receptacle, b: bract, m: marginal flower, t: tube flower). J. Tube flower (p: pappus (calyx), c: corolla, a: anther, s: stigma, st: style), K. Unfertile seed with pappus, L. Fertile seed with dry corolla and stigma, M. Dried seed

The pericycle is a unique tissue and in the xylem sector, it is usually a single cell layer located immediately outside the outermost protoxylem tracheary element. Within xylem, pericycle is the site of initiation of lateral root primordia. The pericycle cells in the phloem are also a single layer, but they have a unique identity and behavior. Phloem pericycle cells are in the adjoining vascular cylinder sector but have a much simpler cell cycle control path. These cells divide several times through complete cell cycles, then arrest and never divide again (Rost 2011). The deepest part of the *P. indica* root is the transport tissue, which consists of xylem and phloem arranged radially. Between xylem and phloem, there is a non-conductive tissue (generally parenchymatous tissue) (Figure $2A_2$).

The cross-sectional anatomy of *P. indica* stem shows several tissues, namely epidermis, cortex, vascular bundles, cambium, and pith (Figures $2B_{1-2}$). The outermost layer is epidermis, which is rectangular and very densely packed as *P. lanceolata* (Khan et al. 2010). In the layer below the epidermis, there is a cortex with an irregular shape and a thin cell. Cortical tissue contains parenchyma cells with transport bundles scattered circularly in certain parts of the cortex (Susetyarini et al. 2020). The type of transport vessel is open collateral (Kadereit and Jeffrey 2007), characterized by phloem located on the adaxial side and xylem on the opposite side (Mehdi et al. 2019). A fascicular cambium is located between phloem and xylem (Ilham et al. 2022). Fascicular cambium may contribute additional cells to both xylem and phloem (Fosket 1994). In addition to function, xylem and phloem of *P. indic*a L. are composed of different cells. Xylem consists of trachea, tracheid, wooden fiber, and parenchyma (Setjo et al. 2004), while phloem comprises sieve tube, companion cells, and parenchyma (Khan et al. 2010). Pith is the deepest tissue in the stem with the largest cell size among all cell types in the stem.

A cross-section anatomical of *P. indica* L. leaves shows the upper epidermal tissue, lower epidermal tissue, mesophyll, xylem, and phloem (Figures $2C_{1-2}$). The upper and lower epidermal tissue is shaped like a brick construction. The epidermis of the leaves is a solid cell construction shape from a square to a rectangle. The epidermis of *P. indica* leaves is also covered by trichomes as reported by Khan et al. (2010) on *P. lanceolata* and Susetyarini et al. (2020) on similar species. Mesophyll tissue in *P. indica* is dorsiventral type. According to Ivanova and P'yankov (2001), plants with this type of mesophyll have a palisade layer on the adaxial side and a spongy layer on the abaxial side. The palisade tissue is more densely arranged than the spongy tissue, which has a very large distance between cells (Chan et al. 2022). The number of chloroplasts in palisade tissue is much higher than in spongy tissue (Yahia and Carrillo-Lopez 2018). Differences in position, number of cells, and number of chloroplasts can cause differences in the amount of light received in each tissue. Vascular bundles are arranged collaterally and located in the leaf's center. Xylem is located on the adaxial side or parallel to the palisade tissue, while phloem is on the opposite side.

The free-hand section of epidermal tissue and cross-section of *P. indica* leaves revealed the anomocytic stomatal cells (Figures 3A and 3E), glandular cells (Figures 3A and 3C), and trichome cells (Figures 3A, 3B, and 3D). The anomocytic stomatal cells consist of two guard cells and four subsidiary cells (Figure 3E). Similar result is also found in another genus *Pluchea* (King-Jones 2001), *P. lanceolata* (Khan et al. 2010), and Asteraceae members (Tekin and Seyda 2021). Therefore, it is suspected that anomocytic stomata are the ancestor of all types of stomata since it also found in the fossil record of Angiosperms and other seed plants (Glas et al. 2012).

There were two types of trichomes, i.e. glandular trichomes and non-glandular trichomes (Figure 3B). The presence of glandular cells (Figure 3C) and glandular trichome (figure 3D) indicated the secondary metabolite storage in the leaf (Wahyuni et al. 2019). Sharma et al. (2017) stated that anatomical structure was essential for understanding secondary metabolite production in plant organs, tissue, or cell.

DNA barcoding

The *rbcL* and *matK* loci were successfully amplified from *P. indica* using primer for Asteraceae as described by Wahyuni et al. (2019) with different lengths of sequences. The summary of alignment results of *rbcL* using BLAST is presented in Table 1. The four best accessions have a close genetic kinship with the sample plants, namely *P. indica* NC_038194.1, *P. indica* MG452144.1, and the last two different species, although still belonging to the same genus, namely *P. pteropoda* NC_060349.1 and *P. pteropoda* MW554520.1.

Table 1. Summary of alignment results of *rbcL* using BLAST

Scientific name	Max score	Total score	Query cover	E value	Per. ident	Acc. len	Accession
Pluchea indica (L.) Less.	891	891	100%	0.0	99.59%	152298	NC_038194.1
P. indica (L.) Less.	891	891	100%	0.0	99.59%	152298	MG452144.1
P. pteropoda Hemsl. ex F.B.Forbes & Hemsl.	891	891	100%	0.0	99.59%	152300	NC_060349.1
P. pteropoda Hemsl. ex F.B.Forbes & Hemsl.	891	891	100%	0.0	99.59%	152300	MW554520.1
Sonchus arvensis L.	802	802	100%	0.0	96.52%	151967	NC_54161.1
S. asper (L.) Hill	802	802	100%	0.0	96.52%	151849	NC_048510.1
S. oleraceus L.	802	802	100%	0.0	96.52%	151849	NC_048452.1
Chrysanthemum lavandulifolium (Fisch. ex Trautv.) Makino	766	766	100%	0.0	94.89%	170038	MW464198.1
Gynura cusimbua (D. Don) S. Moore	771	771	100%	0.0	94.86%	170121	MW238417.1

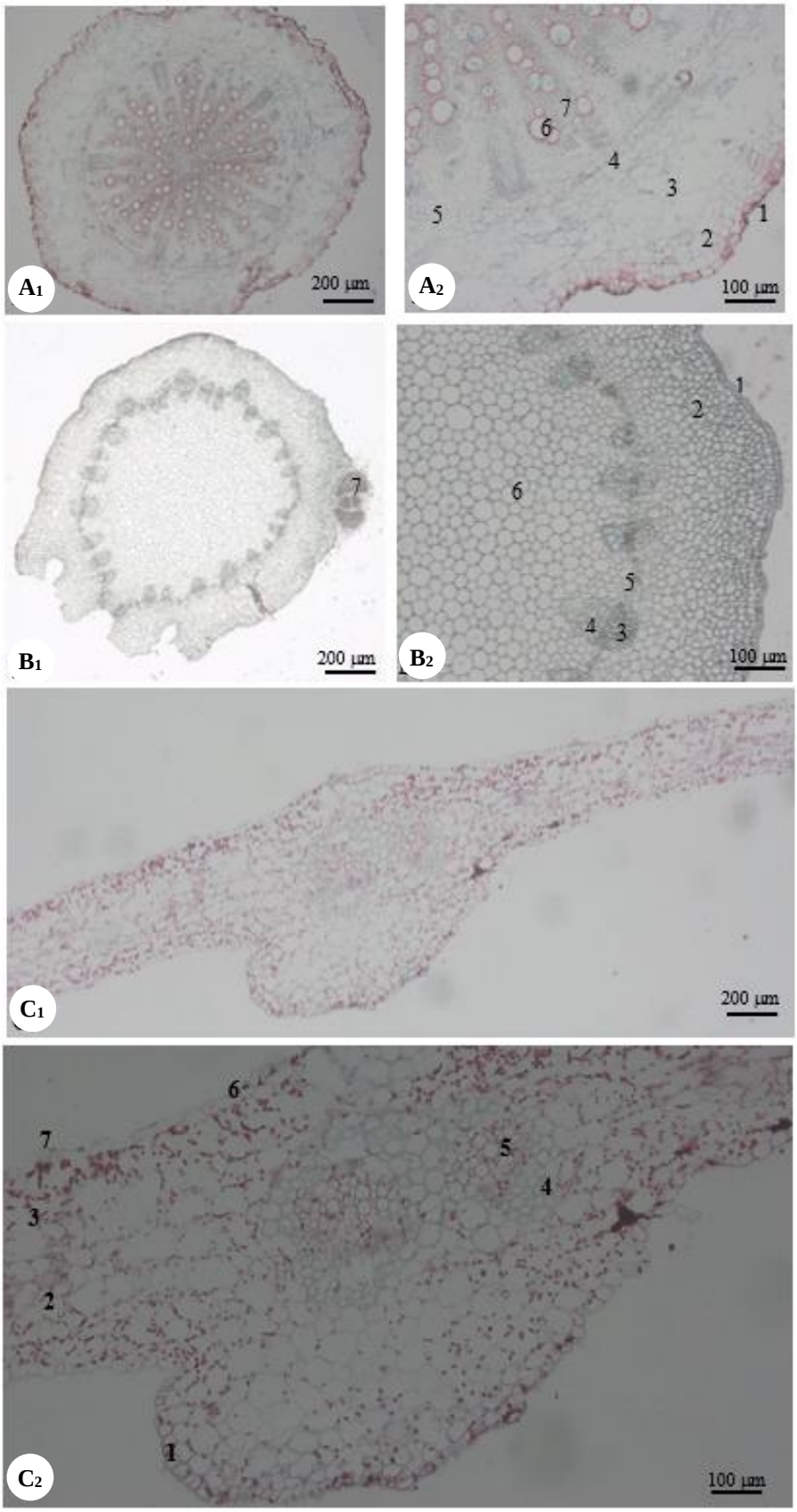

Figure 2. Anatomy of *Pluchea indica* L. (Less.) organs. A_{1-2}. Cross-section of roots 200x and 400x (1: epidermis, 2: collenchyma, 3: cortex, 4: endodermis, 5: pericycle, 6: xylem, 7: phloem). B_{1-2}. Cross section of stems 200 and 400x (1: epidermis, 2: cortex, 3: phloem, 4: xylem, c: Cambium, 6: pith, 7: shoot). C_{1-2}. Cross-section of leaves 200x and 400x (1: lower epidermis, 2: sponge, 3: palisade, 4: phloem, 5: xylem, 6: upper epidermis, 7: stoma)

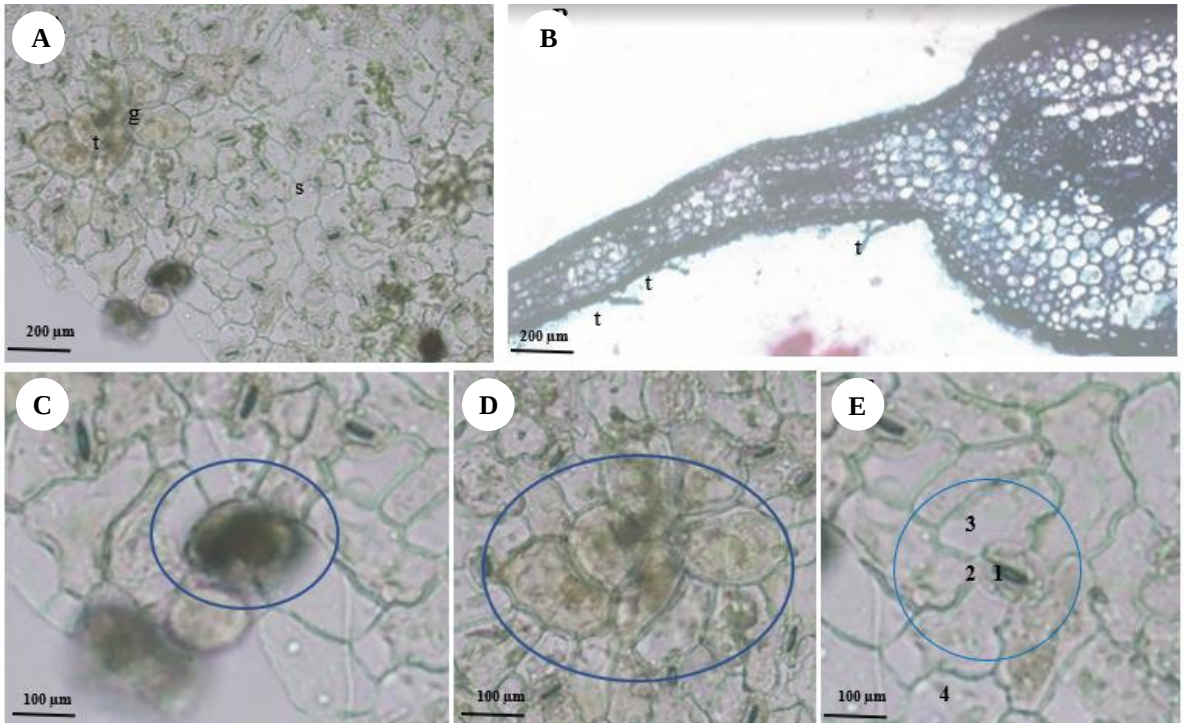

Figure 3. Stomatic and trichome cell of *Pluchea indica* L. (Less.). A. Leaves epidermal tissue 200x (t: trichome, g: glandular cell, s: stomatic cell). B. Transversal section of leaves 200x (t: trichomes). C. Glandular cell 400x. D. Multicellular trichome cell 400x (glandular trichomes). E. Stomatic cell 400x (1: stomatal pore, 2: guard cell, 3: subsidiary cell, 4: epidermal cell)

Alignment of *matK* gene sequences using BLAST showed much greater parameter values than *rbcL* gene-based alignment (Table 2). There were four accessions classified as having high kinship with the sample plants. Two accessions were of the same species (*P. indica* NC_038194.1 and *P. indica* MG452144.1) and two distinct species (*P. pteropoda* NC_060349.1 and *P. pteropoda* MW554520.1).

The *rbcL* sequence of *P. indica* ON685207, *P. indica* ON685208, and *P. indica* ON685209 aligned 477 bases from 736 to 1213 bases compared to the reference *rbcL* gene in *P. indica* MG452144.1. In comparison, the *matK* sequence of *P. indica* ON685204, *P. indica* ON685205, and *P. indica* ON685206 aligned from 488 to 1190 bases against reference *matK* in the exact accession. Percentage coverage of both barcodes was 33.33% and 45.97% for *rbcL* and *matK*, respectively. According to Tindi et al. (2017), the sequence of specimens from the GenBank database has a close genetic relationship with the sample plants if the max score and total score are the same, query cover is close to 100%, e-value is close to 0, and percentage identity is close to 100%.

Phylogenetic tree

The accessions of *P. pteropoda* MW554520.1 and NC_060349.1 became the closest species to *P. indica* based on *rbcL* and *matK* barcodes (Figure 4). *P. indica* MG452144.1 and NC038194.1 were put in the same clade together with *P. pteropoda* in the phylogenetic tree generated by the maximum likelihood tree with GTR + F + G4 as the best fit model and 1000 bootstrap replications. However, *Laggera crispata* OK323148.1 is in the same cluster as *P. indica* and *P. pteropoda* in all phylogenetic trees. Furthermore, the alignment of this full chloroplast genome using NCBI's MEGABLAST indicated that *P. pteropoda* is 99.97% identic to the *P. indica* (NC_038194.1 and MG452144.1). This finding may result in the sequence of our barcode that is misidentified as *P. pteropoda* in NCBI's MEGABLAST hits.

The phylogenetic tree shows the selected barcode's ability to discriminate *P. indica* within Asteraceae (Figure 4). The K2 (Kimura-2 parameter) model was selected for generating a phylogenetic tree of the *rbcL* sequence. The barcode *rbcL* was able to place *P. indica* under study in the same tree as other *P. indica* (MG452144.1 and NC038149.1) in a monophyletic tree (Figure 4A). Two sequences of *P. pteropoda* (NC060349.1 and MW554520) were also clustered together away from *P. indica*'s clade. Unlike the previous alignment using NCBI's MEGABLAST, the phylogenetic tree generated by Maximum likelihood for *rbcL* sequence successfully discriminates *P. indica* from other species within the genus or the family.

Different findings were found in the *matK*-based phylogenetic tree (Figure 4B). The *matK* phylogenetic tree model was only able to distinguish sample plants and *P. indica* from the GenBank database at the genus level, the sample plants had close genetic relationships with *P. pteropoda* (MW554520.1 and NC_060349.1). The phylogenetic tree of *matK* gene was built using the T92 (Tamura 3-parameter) model. High similarity among the *matK* sequence (100% identic) as presented in Table 2 may decrease the ability of this barcode to discriminate within the same genus.

Table 2. Summary of alignment results of *matK* using BLAST

Scientific name	Max score	Total score	Query cover	E value	Per. ident	Acc. len	Accession
Pluchea indica (L.) Less.	1284	1284	100%	0.0	100%	152298	NC_038194.1
P. indica (L.) Less.	1284	1284	100%	0.0	100%	152298	MG452144.1
P. pteropoda Hemsl. ex F.B. Forbes & Hemsl.	891	891	100%	0.0	100%	152300	NC_060349.1
P. pteropoda Hemsl. ex F.B. Forbes & Hemsl.	981	981	100%	0.0	100%	152318	MW554520.1
Sonchus arvensis L.	1118	1118	100%	0.0	95.68%	151967	NC_054161.1
S. asper (L.) Hill	1146	1146	100%	0.0	95.25%	151849	NC_048510.1
S. oleraceus L.	1105	1105	100%	0.0	95.25%	151849	NC_048452.1
Chrysanthemum lavandulifolium (Fisch. ex Trautv.) Makino	704	816	100%	0.0	84.46%	170038	MW464198.1
Gynura cusimbua (D. Don) S. Moore	718	732	100%	0.0	85.16%	170012	MW238417.1

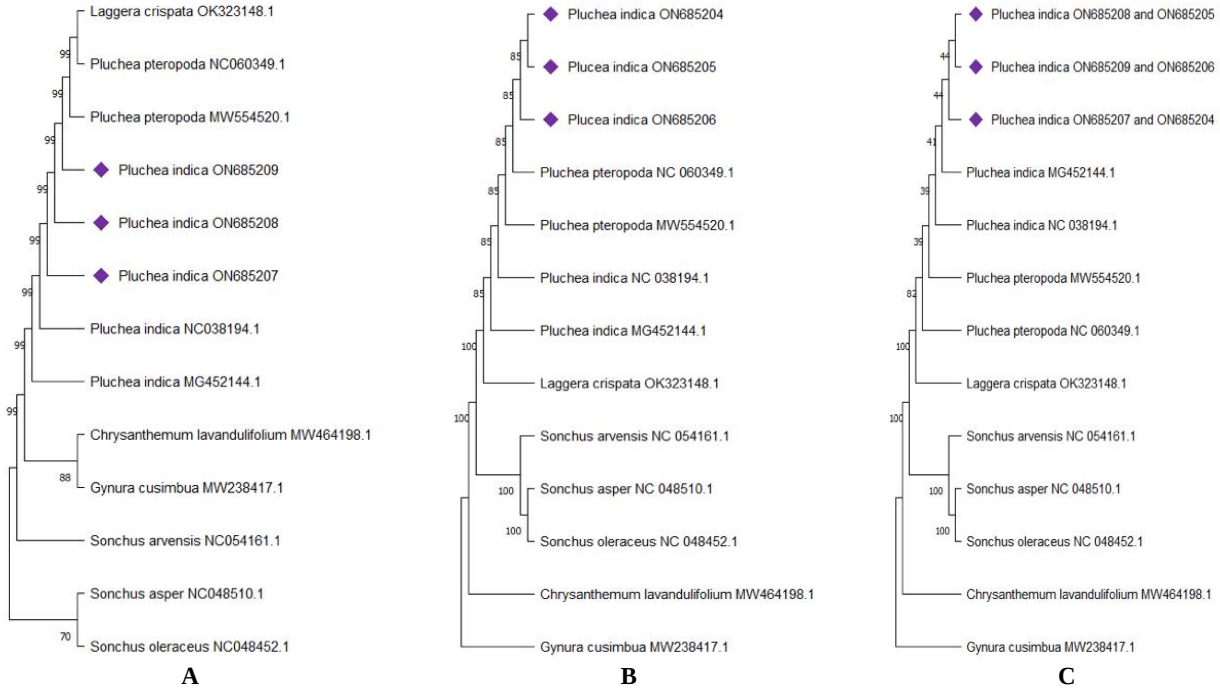

Figure 4. A. Phylogenetic tree of *Pluchea indica* L. (Less.) and several members from Asteraceae is generated by the Maximum Likelihood method of (A) *rbcL* sequence. B. *matK* sequence. C. Combination of *rbcL* + *matK* sequences. Symbol ◊ represents *P. indica* obtained from this study

The last phylogenetic tree is derived from the combination of the *rbcL* and *matK* genes (Figure 4C). This tree has a structure almost similar to the *rbcL* phylogenetic tree (Figure 4A) with a few differences. The difference is in the position of *P. pteropoda*. The position of this species as presented in Figure 4A is relatively closer to the sample plants when compared to Figure 4C. Even though it employed a different best-fit general time reversible model with Gamma distributed and Invariant Sites (GTR+G+I). This model allows unequal rates and base frequencies during the generation of the phylogenetic group.

The molecular approach, such as DNA barcode was conducted to complete the species determination based on morpho-anatomical characters. The evaluation of herbal medicine raw materials is usually based on morphological characters. The morphological examinations of voucher specimens are usually unreliable since depending on human sensory organs (Osathanunkul et al. 2016). Practicing the microscopic level required expert labor. The anatomical examination can identify the sample's origins organ through its unique feature in a specific organ. The structure, density, and distribution of the trichomes can be used to determine the species of a plant and which organ is being observed (Valkama et al. 2003). Nevertheless, the anatomical examination is hardy to deal with dried or grained sample materials.

Medicinal plants have been subjected to DNA barcoding, a new molecular identification, and categorization approach since 2008 (Yu et al. 2021). Single-locus DNA barcode markers such as *rbcL* and *matK* are considered the primary

sequence, while ITS and *trn*H-*psb*A are complementary sequences (CBOL Plant Working Group 2009). It seems like the chloroplast genome becomes favorable rather than the mitochondrion genome like COI as a barcode in the animal kingdom. However, a single-locus barcode may not always provide adequate information, especially at the intraspecific level. The combination of *rbcL* + *matK* could provide better resolution for phylogenetic interference. As a result, a single-locus DNA barcode has a cost advantage, whereas a combined locus can increase identification efficiency (Yu et al. 2021).

Primer pairs successfully amplified the *rbcL* and *matK* gene loci in *P. indica* in this study. This finding is an additional report that these primers can be used in various Asteraceae plants, in addition to being used in *Achillea millefolium* (Ilham et al. 2022) and *Sonchus arvensis* (Wahyuni et al. 2019). The *rbcL* and *matK* gene loci have several pros and cons. In terms of advantages and pros, sometimes in some plant species, heterogeneity is found in these two genes, as evidenced by gaps in certain areas of the nucleotide sequence. The gaps in DNA barcoding can be used to determine whether DNA barcoding will be successful for the taxon under study (Keskin and Atar 2013). The *rbcL* gene has a high amplification success rate (Hollingsworth et al. 2016) although its discriminatory ability at the species level is very low (CBOL Plant Working Group 2009; Gonzalez et al. 2009). Different things happen to the *matK* gene, this gene has a low level of amplification (Sogo et al. 2001; Newmaster et al. 2006; Sass et al. 2007), but the level of species discrimination is very high (Fazekas et al. 2008). Meanwhile, Li et al. (2011) showed that the complement between *rbcL* and *matK* genes provides a very strong resolution power.

On the other hand, using *rbcL* and *matK* genes also has cons and weaknesses. According to Kress and Erickson (2007), using these two gene loci resulted in a low amplification level. Based on the statement of Ho et al. (2021), locus discrimination effectiveness of *rbcL* and *matK* genes varies among plant species, *rbcL* gene has a higher discriminating potential than *matK* for jewel orchids. The statement of Ho et al. (2021) is highly correlated with the current study, in which the *rbcL* gene has excellent discrimination ability down to the species level. The success rate of amplification is also influenced by what organ is used as the DNA source, such as samples from bark are difficult to extract and amplify DNA compared to samples from leaves and roots (Michel et al. 2016). According to Michel et al. (2016), the *rbcL* and *matK* together could not discriminate at the species level, resulting in the polytomy in the phylogenetic tree. The nuclear barcode such as ITS2, on the other hand, can identify the taxonomic identification of the vast majority of the species examined.

Despite the advantage of DNA barcoding in the quality assurance of the herbal product, it is essential to concern several practical notes. Different barcodes from different genomes, such as nuclear, chloroplast, or mitochondrion may involve different rates (Kapli et al. 2020). Moreover, the selection model must accommodate the heterogeneity and substitution rate among the nucleotide sites to reflect the possible phylogenetic tree. The usage of multi-locus DNA barcodes such as concatenated *rbcL* and *matK* must follow the availability deposited sequence in the GenBank since most accession may be available either only *rbcL* or *matK* in the same species. Otherwise, the appropriate interpretation may not be achieved.

In conclusion, morphological characters of *P. indica* are similar to those of Asteraceae plants in general, but the unique characteristics of this plant are the leaves, mainly obovoid leaf, leaf base not decurrent, leaves 1-4 cm wide and 2-7 cm long, and flowers include capitula cylindrical, corolla of disc florets never hair, receptacle glabrous, pappus bristles not fused at base and style long bifid apical sweeping hairs obtuse. Cross sections of anatomical organs showed that the roots, stems, and leaves of *P. indica* had the composition and arrangement of tissues found in dicotyledonous plants in general, but this plant had some specific anatomical characteristics (especially on the leaves) such as anomocytic stomata, glandular cells, and multicellular glandular trichomes. Based on DNA barcoding data processing, genetically the plants studied have a very high similarity with *P. indica* sequences from the GenBank database, which already meet several parameter criteria such as max score and the total score must be the same, query cover is close to 100%, e-value close to 0, percentage identity close to 100% and relationships between specimens based on phylogenetic tree reconstruction.

ACKNOWLEDGEMENTS

We thank Plant Medicinal Garden "*Taman Husada Graha Famili*" Surabaya, East Java, Indonesia for providing plant materials. This study was financially supported by Universitas Airlangga Fiscal Year 2021, following The Decree of the Rector of Universitas Airlangga Number: 794/UN3.15/PT/2021.

REFERENCES

Baas P, Diggle P, Friedman W, Gasson P, Jones C, Wheeler E. 2015. Plant Anatomy: Development, Function, and Evolution. Harvard University, Boston.

Berlin B. 2014. Ethnobiological Classification. Princeton University Press, New Jersey.

CBOL Plant Working Group. 2009. A DNA barcode for land plants. Proc Natl Acad Sci USA 106 (31): 12794-12797. DOI: 10.1016/j.sjbs.2020.08.020.

Chan EWC, Ng YK, Wong SK, Chan HT. 2022. *Pluchea indica*: An updated review of its botany, uses, bioactive compounds, and pharmacological properties. Pharm Sci Asia 49 (1): 77-85. DOI: 10.29090/psa.2022.01.21.113.

De Alba HG. 2015. Development of a DNA barcoding reference library for identification of medicinal plant materials used in the Río Grande Valley of Texas: A representative case study using arnica (Asteraceae). [Thesis]. The University of Texas at Brownsville, Texas.

De Boer HJ, Ouarghidi A, Martin G, Abbad A, Kool A. 2014. DNA barcoding reveals limited accuracy of identifications based on folk taxonomy. PLoS ONE 9 (1): e84291. DOI: 10.1371/journal.pone.0084291.

De Mico MV, Aronne RG. 2012. Morpho-anatomical traits for plant adaptation to drought. In: Aroca R (eds). Plant Responses to Drought Stress. Springer, Berlin/Heidelberg.

Do HDK, Jung J, Hyun JY, Yoon SJ, Lim C, Park K, Kim J-H. 2019. The newly developed single nucleotide polymorphism (SNP) markers

for a potent medicinal plant, *Crepidiastrum denticulatum* (Asteraceae), were inferred from complete chloroplast genome data. Mol Biol Rep 46 (3): 3287-3297. DOI: 10.1007/s11033-019-04789-5.

Dorly D, Wiryo BA, Nurfaizah I, Nidyasari RS. 2015. Secretory structure and histochemistry tests of Asteraceae family members of medicinal plants in Walat Mountain Educational Forest. Proc Biol Educ Conf FKIP UNS 2 (1): 667-673. [Indonesian]

Fazekas AJ, Burgess KS, Kesanakurti PR, Graham SW, Newmaster SG, Husband BC, Percy DM, Hajibabaei M, Barrett SC. 2008. Multiple multilocus DNA barcodes from the plastid genome discriminate plant species equally well. PLoS ONE 3 (7): e2802. DOI: 10.1371/journal.pone.0002802.

Fosket DE. 1994. Plant Growth and Development: A Molecular Approach. Academic Press, San Diego.

Genievskaya Y, Abugalieva S, Zhubanysheva A, Turuspekov Y. 2017. Morphological description and DNA barcoding study of sand rice (*Agriophyllum squarrosum*, Chenopodiaceae) collected in Kazakhstan. BMC Plant Biol 17: 177. DOI: 10.1186/s12870-017-1132.

Glas JJ, Schimmel BC, Alba JM, Escobar-Bravo R, Schuurink RC, Kant MR. 2012. Plant glandular trichomes as targets for breeding or engineering of resistance to herbivores. IntL J Mol Sci 13 (12): 17077-17103. DOI: 10.3390/ijms131217077.

Gonzalez MA, Baraloto C, Engel J, Mori SA, Pétronelli P, Riéra B, Roger A, Thébaud C, Chave J. 2009. Identification of Amazonian trees with DNA barcodes. PLoS ONE 4 (10): e7483. DOI: 10.1371/journal.pone.0007483.

Gratani L. 2014. Plant phenotypic plasticity in response to environmental factors. Adv Bot 2014: 208747. DOI: 10.1155/2014/208747.

Ho VT, Tran TKP, Vu TTT, Widiarsih S. 2021. Comparison of *matK* and *rbcL* DNA barcodes for genetic classification of jewel orchid accessions in Vietnam. J Genet Eng Biotechnol 19 (1): 93. DOI: 10.1186/s43141-021-00188-1.

Hollingsworth PM, Li DZ, van der Bank M, Twyford AD. 2016. Telling plant species apart with DNA: from barcodes to genomes. Philos Trans R Soc Lond B Biol Sci 371 (1702): 20150338. DOI: 10.1098/rstb.2015.0338.

Hong Y, Pandey MK, Lu Q, Liu H, Gangurde SS, Li S, Liu H, Li H, Liang X, Varshney RK, Chen X. 2021. Genetic diversity and distinctness based on morphological and SSR markers in peanuts. Agron J 113: 4648-4660. DOI: 10.1002/agj2.20671.

Hunger S. 1997. A survey of the genus *Pluchea* (Compositae, Plucheeae) in Australia. Willdenowia 27: 207-223. DOI: 10.3372/wi.27.2721.

Ilham M, Mukarromah SR, Rakashiwi GA, Indriati DI, Yoku BF, Purnama PR, Junairiah, Prasongsuk S, Purnobasuki H, Wahyuni DK. 2022. Morpho-anatomical characterization and DNA barcoding of *Achillea millefolium* L. Biodiversitas 23 (4): 1958-1969. DOI: 0.13057/biodiv/d230430.

Ivanova LA, P'Yankov VI. 2001. Structural adaptation of the leaf mesophyll to shading. Russ J Plant Physiol 49 (3): 419-431. DOI: 10.1023/A:1015513607202.

Kadereit G, Jeffrey C. 2007. The Families and Genera of Vascular Plants. Springer-Verlag, Berlin Heidelberg.

Kapli P, Yang Z, Telford MJ. 2020. Phylogenetic tree building in the genomic age. Nat Rev Genet 21 (7): 428-444. DOI: 10.1038/s41576-020-0233-0.

Kaur R, Singh D. 2020. Molecular markers a valuable tool for species identification of insects: A review. Ann Entomol 38 (01-02): 1-20.

Keskin E, Atar HH. 2013. DNA barcoding commercially important fish species of Turkey. Mol Ecol Resour 13 (5): 788-797. DOI: 10.1111/1755-0998.12120.

King-Jones S. 2001. Revision of *Pluchea* Cass. (Compositae, Plucheeae) in the old world. Botanischer Garten und Botanisches Museum, Berlin-Dahlem. Englera 23: 3-136.

Khan S, Rawat R, Rawat AKS, Shirwaiker A. 2010. A report on the quality control parameters of aerial parts of *Pluchea lanceolata* (DC.) Oliv. & Hiern, Asteraceae. Rev Bras Pharmacogn 20 (4): 563-567. DOI: 10.1590/S0102-695X2010000400015.

Leroux O. 2012. Collenchyma: A versatile mechanical tissue with dynamic cell walls. Ann Bot 110 (6): 1083-1098. DOI: 10.1093/aob/mcs186.

Li FW, Kuo L-Y, Rothfels CJ, Ebihara A, Chiou W-L, Windham MD, Pryer KM. 2011. RbcL and matK earn two thumbs up as the core DNA barcode for ferns. PLoS ONE 6 (10): e26597. DOI: 10.1371/journal.pone.0026597.

Kress WJ, Erickson DL. 2007. A two-locus global DNA barcode for land plants: The coding *rbcL* gene complements the non-coding trnH-psbA spacer region. PLoS ONE 2 (6) :e508. DOI: 10.1371/journal.pone.0000508.

Kress WJ, Erickson DL, Jones FA, Swenson NG, Perez R, Sanjur O, Bermingham E. 2009. Plant DNA barcodes and a community phylogeny of a tropical forest dynamics plot in Panama. Proc Natl Acad Sci USA 106 (44): 18621-18626. DOI: 10.1073/pnas.0909820106.

Kress WJ. 2017. Plant DNA barcodes: Applications today and in the future. J Syst Evol 55 (4): 291-307. DOI: 10.1111/jse.12254. 17.

Kumar S, Stecher G, Li M, Knyaz C, Tamura K. 2018. MEGA X: Molecular evolutionary genetics analysis across computing platforms. Mol Biol Evol 35 (6): 1547-1549. DOI: 10.1093/molbev/msy096.

Mandel JR, Dikow RB, Siniscalchi CM, Thapa R, Watson LE, Funk VA. 2019. A fully resolved backbone phylogeny reveals numerous dispersals and explosive diversifications throughout the history of Asteraceae. Proc Natl Acad Sci USA 16 (28): 14083-14088. DOI: 10.1073/pnas.1903871116.

Mao X, Xie W, Li X, Shi S, Guo Z. 2021. Establishing community-wide DNA barcode references for conserving mangrove forests in China. BMC Plant Biol 21 (1): 571. DOI: 10.1186/s12870-021-03349-z.

Mehdi R, Lamm CE, Anjanappa RB, Mudsam C, Saeed M, Klima J, Kraner ME, Ludewig F, Knoblauch, Gruissem W, Sonnewald U, Zierer W. 2019. Symplasmic phloem unloading and radial post-phloem transport via vascular rays in tuberous roots of *Manihot esculenta*. J Exp Bot 70 (20): 5559-5573. DOI: 10.1093/jxb/erz297.

Mercado MI, Marcial G, Catalan JV, Grau A, Catalan CAN, Ponessa GI. 2021. Morphoanatomy, histochemistry, essential oil, and other secondary metabolites of *Artemisia copa* (Asteraceae). Bot Lett 68 (4): 577-593. DOI: 10.1080/23818107.2021.1956585.

Michel CI, Meyer RS, Taveras Y, Molina J. 2016. The nuclear internal transcribed spacer (ITS2) as a practical plant DNA barcode for herbal medicines. J Appl Res Med Aromat Plants 3 (3): 94-100. DOI: 10.1016/j.jarmap.2016.02.002.

Miyashima S, Nakajima K. 2011. The root endodermis: A hub of developmental signals and nutrient flow. Plant Signal Behav 6 (12): 1954-1958. DOI: 10.4161/psb.6.12.18079.

Newmaster SG, Fazekas AJ, Ragupathy S. 2006. DNA barcoding in land plants: Evaluation of *rbcL* in a multigene tiered approach. Can J Bot 84 (3): 335-341. DOI: 10.1139/b06-047.

Osathanunkul K, Madesis P, de Boer H. 2016. Evaluation of DNA barcoding coupled high resolution melting for discrimination of closely related species in phytopharmaceuticals. Phytomed 23 (2): 156-165. DOI: 10.1016/j.phymed.2015.11.018.

Patwardhan A, Ray S, Roy A. 2014. Molecular markers in phylogenetic studies - A review. J Phylogen Evol Biol 2 (2): 1-9. DOI: 10.4172/2329-9002.1000131.

Peng C-I, Chen C-H, Leu W-P, Yen H-F. 1998. *Pluchea* Cass. (Asteraceae: Inuleae) in Taiwan. Bot Bull Acad Sin 39: 287-297.

Purnobasuki H, Purnama PR, Kobayashi K. 2017. Morphology of four root types and anatomy of root-root junction in relation gas pathway of *Avicennia marina* (Forsk) Vierh roots. Vegetos 30 (2): 100-104. DOI: 10.5958/2229-4473.2017.00143.4.

Rost TL. 2011. The organization of roots of dicotyledonous plants and the positions of control points. Ann Bot 107: 1213-1222. DOI: 10.1093/aob/mcq229.

Santos RF, Nunes BM, Sá RD, Soares LAL, Randau KP. 2016. Morpho-anatomical study of *Ageratum conyzoides*. Rev Bras Farmacogn 26 (6): 679-687. DOI: 10.1016/j.bjp.2016.07.002.

Sass C, Little DP, Stevenson DW, Specht CD. 2007. DNA barcoding in the Cycadales: Testing the potential of proposed barcoding markers for species identification of cycads. PLoS ONE 2 (11): e1154. DOI: 10.1371/journal.pone.0001154.

Sarvananda L. 2018. Short introduction of DNA Barcoding. Intl J Res 5 (4): 673-686.

Setjo S, Kartini E, Saptasari M, Sulisetijono. 2004. Plant Anatomy. Universitas Negeri Malang, Malang. [Indonesian]

Sharma S, Richa, Harsimran. 2017. Phytochemical and anatomical screening of *Ecliptca prostrata* L. an important medical herb from Chandigarh. J Med Plants Stud 5 (2): 255-258.

Simpson MG. 2006. Plant Systematic. Academic Press, Amsterdam.

Srisook K, Jinda S, Srisook E. 2021. Anti-inflammatory and antioxidant effects of *Pluchea indica* leaf extract in TNF-α-induced human endothelial cells. Walailak J Sci Technol 18 (10): 1-12. DOI: 10.48048/wjst.2021.10271.

Sogo A, Setoguchi H, Noguchi J, Jaffre T, Tobe H. 2001. Molecular phylogeny of Casuarinaceae based on *rbcL* and *matK* gene sequences. J Plant Res 114 (4): 459-464. DOI: 10.1007/PL00014011.

Sugiaman VK, Nisyah NQ, Anisa N, Pranata N. 2021. *Pluchea indica* extract as a potential source of nutrition for accelerate wound healing. Syst Rev Pharm 12 (1): 570-573. DOI: 10.31838/srp.2021.1.82.

Suriyaphan O. 2014. Nutrition, health benefits, and applications of *Pluchea indica* (L.) Less. leaves. Mahidol Univer J Pharm Sci (Pharm Sci Asia) 41 (4): 1-10.

Susetyarini E, Wahyono P, Latifa R, Nurrohman E. 2020. The identification of morphological and anatomical structures of *Pluchea indica*. J Phys Conf Ser 1539: 012001. DOI: 10.1088/1742-6596/1539/1/012001.

Tamura K, Stecher G, Kumar S. 2021. MEGA11: Molecular evolutionary genetics analysis version 11. Mol Biol Evol 8 (7): 3022-3027. DOI: 10.1093/molbev/msab120.

Tekin M, Seyda A. 2021. Anatomical investigations of the Turkish critically endangered species: *Achillea sivasica* Çelik et Akpulat (Asteraceae). Acta Bot Croat 80 (1): 91-98. DOI: 10.37427/botcro-2021-006.

Tindi M, Mamangkey NGF, Wullur S. 2017. The DNA barcode and molecular phylogenetic analysis several bivalve species from North Sulawesi waters based on COI gene. Jurnal Pesisir dan Laut Tropis 1 (2): 33-38. DOI: 10.35800/jplt.5.2.2017.15050. [Indonesian]

Ulrich-Merzenich G, Zeitler H, Jobst D, Panek D, Vetter H, Wagner H. 2007. Application of the "-Omic-" technologies in phytomedicine. Phytomedicine 14 (1): 70-82. DOI: 10.1016/j.phymed.2006.11.011

Valkama E, Salminen JP, Koricheva J, Pihlaja K. 2003. Comparative analysis of leaf trichome structure and composition of epicuticular flavonoids in Finnish birch species. Ann Bot 91 (6): 643-655. DOI: 10.1093/aob/mcg070.

Veeresham C. 2012. Natural products derived from plants as a source of drugs. J Adv Pharm Technol Res 3 (4): 200-201. DOI: 10.4103/2231-4040.104709.

Wahyuni DK, Ekasari E, Witono JR, Purnobasuki H. 2016. Toga Indonesia. Airlangga University Press. Surabaya. [Indonesian]

Wahyuni DK, Rahayu S, Purnama PR, Saputro TB, Suharyanto, Wijayanti N, Purnobasuki H. 2019. Morpho-anatomical structure and DNA barcode of *Sonchus arvensis* L. Biodiversitas 20 (8): 2417- 2426. DOI: 10.13057/biodiv/d200841.

Wilson TC, Conn BJ, Henwood MJ. 2017. Great expectations: Correlations between pollinator assemblages and floral characters in Lamiaceae. J Plant Sci 178 (3): 170-187. DOI: 10.1086/690023170.

Yahia E, Carrillo-Lopez A. 2018. Postharvest Physiology and Biochemistry of Fruits and Vegetables. Woodhead Publishing, Cambridge.

Yang J, Vázquez L, Chen X, Li H, Zhang H, Liu Z, Zhao G. 2017. Development of chloroplast and nuclear DNA markers for Chinese oaks (*Quercus* Subgenus *Quercus*) and assessment of their utility as DNA Barcodes. Front Plant Sci 8: 816. DOI: 10.3389/fpls.2017.00816.

Yu J, Wu X, Liu C, Newmaster S, Ragupathy S. Kress WJ. 2021. Progress in the use of DNA barcodes in the identification and classification of medicinal plants. Ecotoxicol Environ Saf 208: 111691. DOI: 10.1016/j.ecoenv.2020.111691.

Zagoto ADP, Violita V. 2019. Leaf anatomical modification in drought of rice varieties (*Oryza sativa* L.). Eksakta 20 (2): 42-52. DOI: 10.24036/eksakta/vol20-iss2/201.